

**EUTROPHICATION:  
RESEARCH AND APPLICATION TO WATER SUPPLY**

Edited by

**DAVID W. SUTCLIFFE AND J. GWYNFRYN JONES**

Published by the Freshwater Biological Association

Invited papers from a specialised conference held in London  
on 10-11 December 1991 by the  
Freshwater Biological Association,  
The Ferry House, Far Sawrey, Ambleside, Cumbria LA22 0LP  
and  
International Water Supply Association,  
1 Queen Anne's Gate, London SW1H 9BT

© Freshwater Biological Association 1992

ISBN 0-900386-52-5

# The impact of physical processes on algal growth

DIETER M. IMBODEN

*Swiss Federal Institute of Technology, Swiss Federal Institute for  
Water Resources and Water Pollution Control, CH-8600, Dübendorf, Switzerland*

Mixing and transport processes in surface waters strongly influence the structure of aquatic ecosystems. The impact of mixing on algal growth is species-dependent, affecting the competition among species and acting as a selective factor for the composition of the biocoenose. Were it not for the ever-changing "aquatic weather", the composition of pelagic ecosystems would be relatively simple. Probably just a few optimally adapted algal species would survive in a given water-body.

In contrast to terrestrial ecosystems, in which the spatial heterogeneity is primarily responsible for the abundance of niches, in aquatic systems (especially in the pelagic zone) the niches are provided by the temporal structure of physical processes. The latter are discussed in terms of the relative sizes of physical versus biological time-scales. The relevant time-scales of mixing and transport cover the range between seconds and years. Correspondingly, their influence on growth of algae is based on different mechanisms: rapid changes are relevant for the fast biological processes such as nutrient uptake and photosynthesis, and the slower changes are relevant for the less dynamic processes such as growth, respiration, mineralization, and settling of algal cells. Mixing time-scales are combined with a dynamic model of photosynthesis to demonstrate their influence on algal growth.

---

## Introduction

It is well-known that plants living on land are strongly influenced by climatic factors, such as precipitation, air temperature, solar radiation, wind speed and others. These factors, together with the chemical properties of the soil, are the major factors which determine the competition between different plant species and the composition of the terrestrial ecosystem.

It may be less obvious that in aquatic ecosystems the situation is quite similar: algal competition is controlled by the combined action of the chemistry of the water and the "aquatic weather", i.e. the physical processes in the water column. Obviously, there are some important differences between the terrestrial and aquatic climate. Firstly, precipitation cannot be a selective factor for the aquatic system. Secondly, water currents are not analogues of terrestrial winds, as most organisms living in the pelagial region of aquatic ecosystems are freely floating. Therefore, water currents are not primarily a stress factor, in the way that terrestrial winds affect plants, but the currents are agents of movement which transport the living cells from one region to another, e.g. from light to dark zones and *vice versa*.

The impact of mixing and transport processes on algal growth is species-dependent, affecting the competition among species and acting as a selective factor for the composition of the biocoenose. Were it not for the ever-changing "aquatic weather", the composition of pelagic ecosystems would be relatively simple. Probably just a few optimally adapted algal species would survive in a given water-body.

In contrast to terrestrial ecosystems, in which the *spatial heterogeneity* is primarily responsible for the abundance of niches, in aquatic systems (especially in the pelagic zone) the

niches are provided by the *temporal structure* of physical processes. The important characteristic quantity is the relative size of physical versus biological time-scales. The relevant time-scales of mixing and transport cover the range between seconds and years (Imboden 1990). Correspondingly, their influence on growth of algae is based on different mechanisms: rapid changes are relevant for the fast biological processes such as nutrient uptake and photosynthesis, and the slower changes are relevant for the less dynamic processes such as growth, respiration, mineralization, and settling of algal cells.

Figure 1 gives a simplified sketch of the relationship between physical processes in lakes and algal population growth. Obviously, the situation is far too complex to be exhaustively covered in a short review article. Therefore, two types of mechanisms will be chosen in order to exemplify a situation which actually is extremely complicated and not yet understood in every detail. The first mechanism is related to the long-term balance of biomass and nutrients in the trophogenic (productive) surface layer. Here we are looking at processes controlling the nutrient and algal concentrations which in turn are directly influencing algal growth. We shall call this the *capacity limitation* of growth. The second mechanism is given by the short-term processes of mixing, which causes individual algal cells to continuously change their depth and thus the light intensity to which they are exposed. The corresponding response of photosynthesis to temporal changes of light is called *dynamic limitation* of growth.

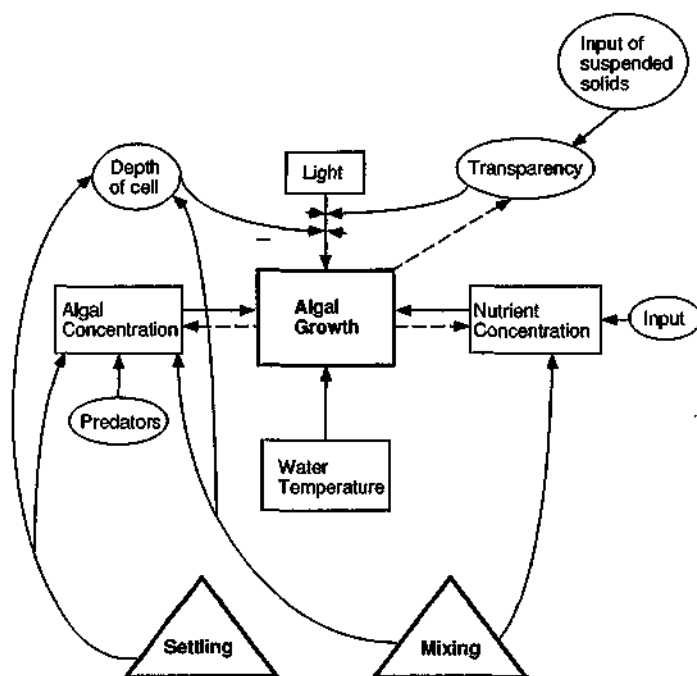


Figure 1. Schematic diagram to show the relations between algal growth and physical processes in lakes represented by the two major transport phenomena, (particle) "settling" and "mixing".

### Capacity limitation: Long-term physical processes

Photosynthesis depends on the presence of two types of resources, i.e. light and nutrients. While the former is restricted to the water layers close to the surface, nutrients tend to be depleted in the productive zone, leading to a steady-state in which internal recycling and inputs

from outside are balanced by uptake of nutrients by algae. This simple balance represents one important control mechanism for the overall capacity of the biological productivity in the system.

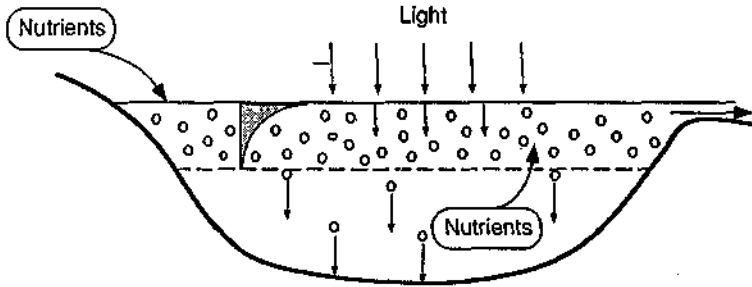


Figure 2. Epilimnetic mass balance for nutrients. The nutrient concentration (nitrate, phosphate, etc.) in the trophogenic layer is influenced by external loading, internal diffusion from the hypolimnion, settling of biomass, and loss through the outlet. The depth of the trophogenic layer is controlled by the light extinction in the water column and thus is generally smaller in waters with large biomass concentrations.

Let us discuss the problem of capacity limitation in a quantitative manner by considering a very simple mass balance scheme for nutrients in the trophogenic layer (Fig. 2). For a simple box model (trophogenic layer is completely mixed) the following equations can be formulated:

$$\frac{dN}{dt} = J_e + J_i - E_N - G + R \quad (1)$$

$$\frac{dB}{dt} = E_B + G - R \quad (2)$$

where  $N$  is the mean nutrient concentration in the trophogenic layer,  $B$  is the mean biomass concentration expressed as the concentration of nutrient  $N$  incorporated in the biomass,  $J_e$  is the external input of nutrient,  $J_i$  is the internal input of nutrients by vertical mixing through the thermocline,  $E_N$  is loss of nutrient from the layer by transport,  $E_B$  is loss of biomass from the layer by transport,  $R$  is loss of biomass from the layer by respiration or mineralization, and  $G$  is uptake of nutrient by the biomass.

Note that all variables appearing on the right hand side of eqns (1) and (2) are expressed as change of mass per unit time and volume.

In a greatly simplified way nutrient uptake, photosynthesis and algal growth can all be considered as synonyms, at least for long-term considerations for which changes of the stoichiometric composition of the biomass are less important than for short-term processes. If  $N$  is the limiting nutrient, algal growth per unit area,  $\Sigma G$ , expressed by the combined Michaelis-Menten/self-saturation equation, is given by (Imboden & Gächter 1978):

$$\Sigma G = hG = \mu \frac{N}{K_N + N} \frac{B}{\epsilon_0 + \beta B} \quad (3)$$

where  $\mu$  is the maximum growth rate,  $K_N$  is the Michaelis constant for nutrient  $N$ ,  $\epsilon_0$  is the light extinction coefficient for water without biomass,  $\beta$  is the biomass-specific increase of extinction coefficient, and  $h$  is the depth of mixed layer.

All the other terms shall be expressed by first-order processes, i.e.

$$E_N = k_w N \quad (4)$$

the loss of nutrient through the outlet, where  $k_w$  is the flushing rate of the mixed layer;

$$E_B = (k_w + k_s) B \quad (5)$$

the loss of biomass through the outlet and by settling, where  $k_s$  is the settling rate;

$$R = k_r B \quad (6)$$

the degradation of biomass by respiration or mineralization, where  $k_r$  is the respiration/mineralization rate.

Inserting the expressions (3) to (6) into eqns (1) and (2), and solving for steady-state, yields a functional relationship between the productivity per unit area and time,  $\Sigma G$ , and the total nutrient input to the trophogenic layer,  $J_e + J_i$ . The term  $\Sigma G$  can be decomposed into the "minimum" production,  $\Sigma G_o$ , which holds if no nutrients from the hypolimnion are recycled ( $J_i = 0$ ), and the additional production,  $\Delta G_i$ , originating from the internal nutrient supply  $J_i$ . Thus

$$\Sigma G = \Sigma G_o + \Sigma G_i \quad (7)$$

Note that in  $\Sigma G$  the much faster epilimnic phosphorus uptake and release is not taken into account but only the net phosphorus uptake which, over longer periods, acts in parallel with carbon uptake and thus with algal growth. An average Redfield factor of 40g C versus 1g P is used to convert  $\Sigma G$  into carbon uptake,  $\Sigma G^C$ . Mixing depth ( $h$ ) and production rate ( $\Sigma G$ ) show significant seasonal variations, with the result that most of the yearly productivity occurs during the stagnation period, i.e. during about eight months. In a simplified way, the annual primary productivity is calculated from the steady-state concentrations  $N_{ss}$  and  $B_{ss}$ :

$$\Sigma G_o^C = 40 (T_{St} \times \mu_{St}) \left( \frac{N_{ss}}{k_N + N_{ss}} \right) \left( \frac{B_{ss}}{\epsilon_o + \beta B_{ss}} \right) \quad (8)$$

where  $T_{St}$  is 240 days per year, the average duration of the stagnation period, and  $\mu_{St}$  is the mean uptake rate during this period. Average parameter values from Imboden & Gächter (1978) are listed in Table 1. The calculated variation of  $\Sigma G_o^C$  as a function of external loading per unit area and time,  $L_P = hJ_e$ , is very similar to the lower boundary of measured values (Fig. 3).

Table 1. Definitions and values of parameters for a simple phosphorus lake-model (From Imboden & Gächter 1978)

Symbol	Values and Units	Definitions
$N$	mg m <sup>-3</sup>	concentration of dissolved nutrient (e.g. phosphorus)
$B$	mg m <sup>-3</sup>	concentration of biomass, expressed as particulate nutrient
$L_P$	mg P m <sup>-2</sup> yr <sup>-1</sup>	annual P-input in lake per unit surface area
$h$	6 m	depth of trophogenic layer
$k_w$	yr <sup>-1</sup>	exchange of epilimnic water by river inlets and outlets
$k_r$	0.07 d <sup>-1</sup>	rate constant of mineralization of organic material
$k_s$	0.025 d <sup>-1</sup>	loss of biomass from epilimnion by sedimentation
$G$	mg P m <sup>-2</sup> d <sup>-1</sup>	P-uptake taken as measure for primary production
$\mu$	1 d <sup>-1</sup>	maximum P-uptake rate
$K_N$	1.5 mg P m <sup>-3</sup>	Michaelis constant for nutrient $N$
$\epsilon_o$	0.3 m <sup>-1</sup>	extinction coefficient of water without biomass
$\beta$	0.015 m <sup>-2</sup> (mg P) <sup>-1</sup>	specific influence of biomass on extinction
$\Sigma G$	mg P m <sup>-2</sup> yr <sup>-1</sup>	uptake of P per unit time and water column
$\Sigma G^C$	mg C m <sup>-2</sup> yr <sup>-1</sup>	carbon uptake (assumed Redfield ratio $\Sigma G^C = 40 \Sigma G$ )

The role of internal phosphorus supply becomes more evident by using the so-called P-efficiency,  $n_p$ , defined as the average number of times each phosphorus atom takes part in the photosynthetic process before leaving the lake through the outlet or permanent incorporation into the sediments:

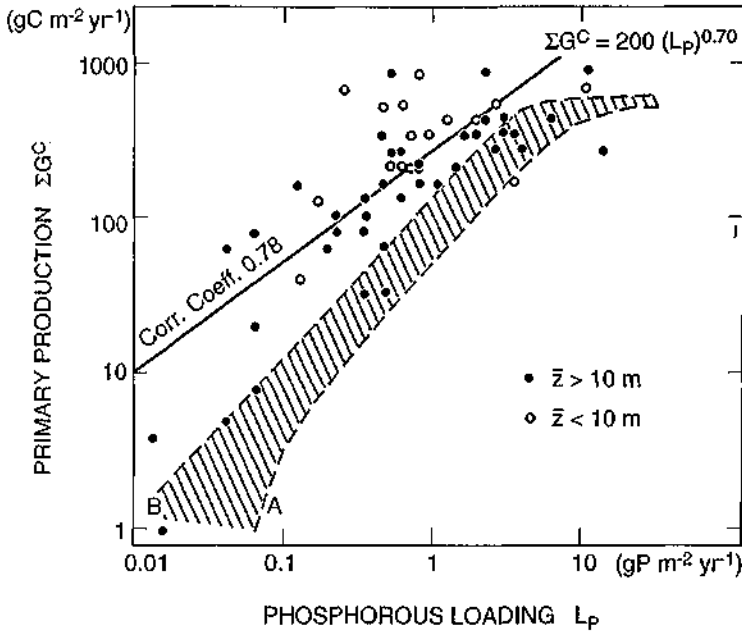


Figure 3. Relationship between external annual P-loading per unit surface area,  $L_p$ , and primary productivity  $\Sigma G^C$ , for various European and North-American lakes, taken from the OECD eutrophication program (Vollenweider & Kerekes 1982). The shaded area was calculated with eqn (8) for epilimnic water-residence times ( $1/k_w$ ) between 0.06 years (curve A) and 15 years (curve B). Shallow lakes (mean depth  $\bar{z} < 10 \text{ m}$ ) show a slight tendency towards larger productivities, indicating a possible influence from internal nutrient loading,  $J_i$ . From Imboden & Gächter (1979).

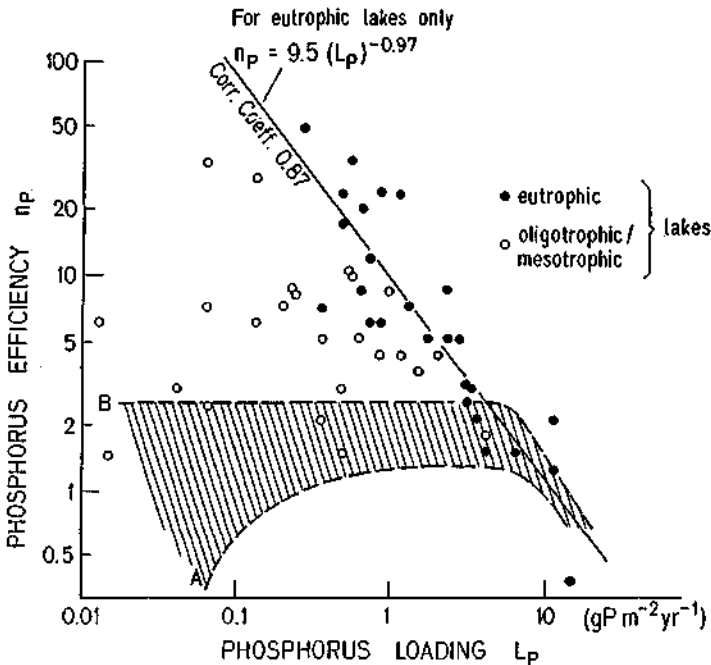


Figure 4. Phosphorus efficiency,  $n_p$  (eqn 9), as a function of P-loading,  $L_p$ . The shaded area (curves A and B) was calculated from the steady-state model, as explained in Fig. 3. From Imboden & Gächter (1979).

$$n_P = \Sigma G / L_P = \frac{\Sigma G^c}{40 (L_P)} \quad (9)$$

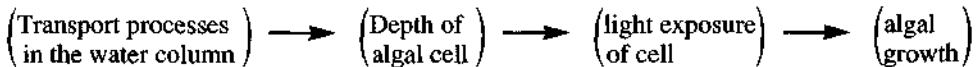
In Figure 4, values of measured  $n_P$  are plotted (for the same set of lakes as in Fig. 3) and compared to  $n_P$  values computed from the steady-state model (eqn 8). For large values of  $L_P$ , measured values agree with the steady-state model, indicating that  $\Sigma G$  is controlled by light (self-shadowing), while internal nutrient recirculation does not influence such lakes which are too richly nourished already.

The scattering of the  $n_P$  values as a function of  $L_P$  is significantly reduced if only eutrophic lakes are considered. The linear regression found between  $\log L_P$  and  $\log n_P$  for eutrophic lakes is nearly identical with the relation:  $\Sigma P = 380 \text{ g C m}^{-2} \text{ year}^{-1}$ . In other words, primary productivity in these eutrophic lakes seems to be remarkably independent of  $L_P$  and has a mean value of about  $400 \text{ g C m}^{-2} \text{ year}^{-1}$ .

The important message here is that the difference between the minimum (externally driven) growth as calculated by the model, and the measured growth, reflects the role of internal nutrient supply by mixing. However, mean depth alone cannot explain the magnitude of  $\Sigma G_i$ ; probably other factors such as lake morphometry, exposure to wind, and chemical processes occurring at the sediment-water interface are of comparable importance.

#### Dynamic limitation: short-term physical processes

In this section the following dynamic sequence of causes and effects will be considered:



In this context our interest will be focused on the vertical motions in the water. Since in most cases, especially during the period of greatest algal productivity, lakes are vertically stratified, the vertical motion of the water is greatly damped by buoyancy effects. Figure 5 shows two kinds of vertical motion: (1), the reversible excursion of isopycnals (surfaces of constant water density  $\rho_A$ ,  $\rho_B$ , etc.) about their equilibrium depths (designated as  $\rho_A^0$ ,  $\rho_B^0$ , etc.) as caused by internal waves and seiches, and (2), the irreversible mixing of the water across the isopycnals due to turbulent mixing.

#### Reversible motion

Because of the kinetic energy input by winds and inlets, isopycnals are hardly ever at rest. The long standing waves found in closed basins, called internal seiches (Mortimer 1974), are often only weakly damped and can therefore store wind energy over long time-periods (Fig. 6). Typical vertical amplitudes are in the order of 1 to 2 metres, corresponding to relative variations of light intensity by a factor of 2 to 10. (Note: Take  $e^{\epsilon \Delta z}$  with light extinction  $\epsilon = 0.3$  to  $0.5 \text{ m}^{-1}$  and  $\Delta z = 1$  to  $2 \text{ m}$ ). During extreme situations (e.g. storm events) vertical isopycnal displacements can reach 40 m and more in just a few hours (Fig. 7).

The complex temporal variation of isopycnal depth can be analyzed by spectral analysis in order to identify the most important time-scales of motion. As shown in Figure 8, most energy is concentrated in the relatively slow standing waves (seiches). However, at the higher frequency end of the spectrum, which is not sufficiently resolved by the data used to calculate the spectra shown in Figure 8, one can often find distinct maxima (Fig. 9). They represent the so-called stability frequency defined by

$$N = \left( \frac{g}{\rho} \frac{d\rho}{dz} \right)^{1/2} \quad (10)$$

where  $g$  is acceleration of gravity ( $9.81 \text{ m s}^{-2}$ ) and  $d\rho/dz$  is the vertical density gradient in the water column.

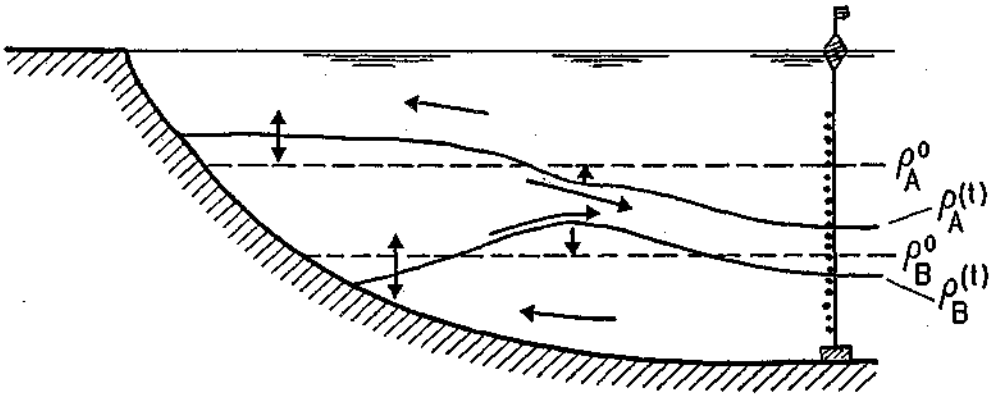


Figure 5. Two types of vertical motion in lakes: a reversible excursion of isopycnals (surfaces of constant water density),  $\rho_A, \rho_B \dots$  about their equilibrium position,  $\rho_A^0, \rho_B^0 \dots$  (shown by single arrows), and irreversible mixing of water across isopycnals by turbulence (shown by double arrows).

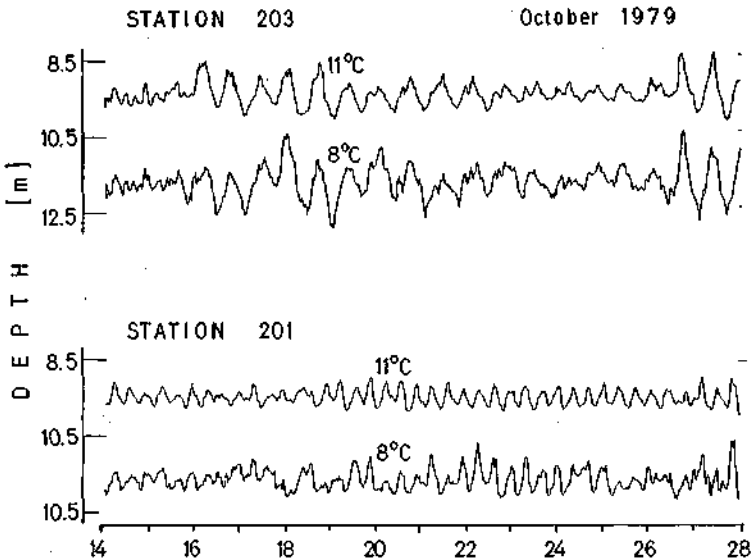


Figure 6. Vertical oscillations of isotherms in Lake Baldegg (Switzerland). Damping is small so that oscillation survives between wind events (e.g. from 19 October to 26 October). From Imboden *et al.* (1983).

The corresponding period  $T = 2\pi/N$ , depends on the strength of the stratification. In the thermocline during the summer,  $T$  is of the order of a few minutes. As will be discussed below, this time-scale is of the same order as the response of the planktonic photosynthesis to changing light intensities.



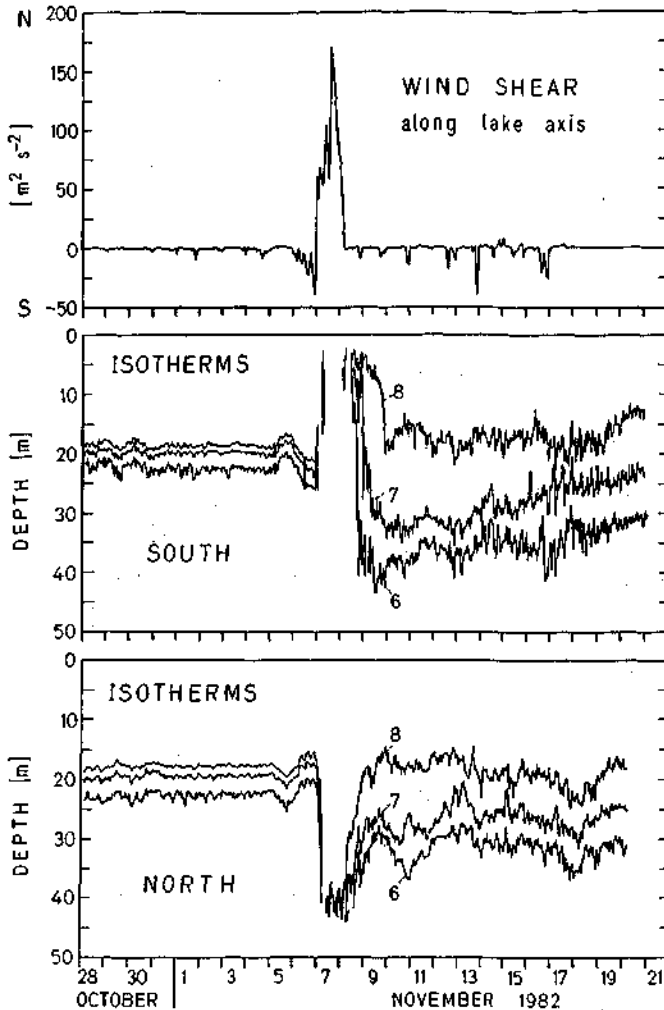


Figure 7. Directed wind shear ( $m^2 s^{-2}$ ) along the main axis of Lake Zug (Switzerland) and isotherm depths (m) at two stations, North and South, demonstrate the influence of a severe storm on 7/8 November 1982. From Imboden *et al.* (1988).

#### *Irreversible motion*

Turbulence leads to irreversible mixing between adjacent water layers and to irreversible vertical displacements of the suspended plankton. The dynamics of turbulence in the uppermost layers is driven by two processes, wind mixing and heat exchange. For water temperatures above the density maximum (at about  $4^\circ C$  for fresh water), warming causes the water column to become more stable while cooling leads to convective mixing, even in the absence of any wind. In fact, cooling occurs during most nights of the year (Marti & Imboden 1986), while during most days (except at low air temperature in the winter) the water column gains some heat. The diurnal change of the direction of the heat flux between water and atmosphere causes a diurnal stabilization/mixing rhythm which becomes even more complex by the additional influence from the wind.

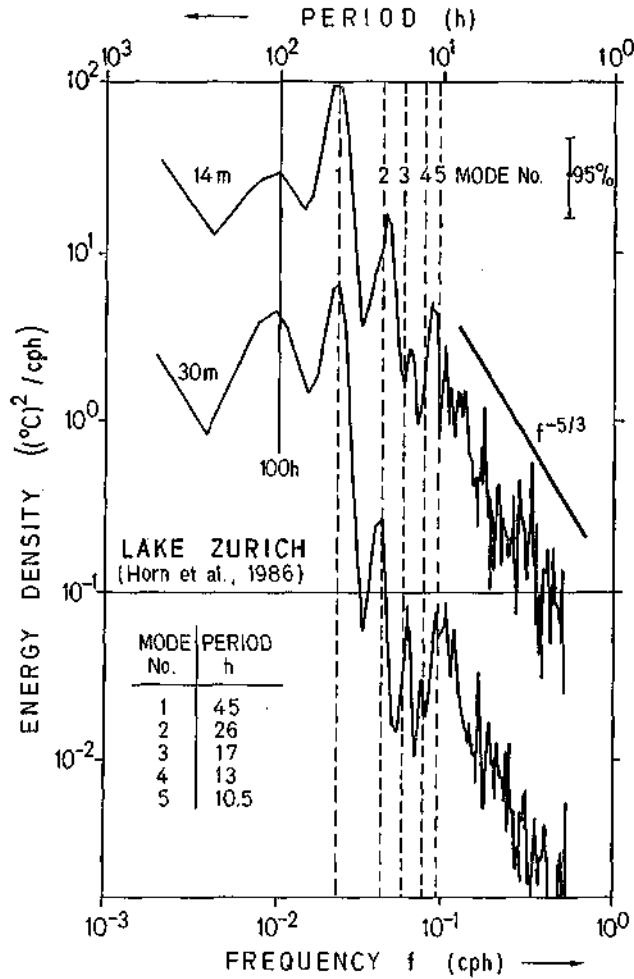


Figure 8. Spectra of fluctuations of hourly mean temperature in Lake Zürich (Switzerland) for a period of 1000 hours. The peaks denoted as mode no. 1 to 5 are standing internal waves (seiches). From Horn *et al.* (1986).

During the day, wind and heat flux usually act against each other: the heat flux suppresses vertical mixing and the wind drives it. The Monin-Obukhov length,  $L$ , is a measure for the interplay between wind and heat flux. It defines the depth to which the water would eventually be mixed if heat flux and wind persistently remained constant. As can be seen in Figure 10,  $L$  is shallow for small wind speeds and large heat fluxes (e.g. 5 May 1983, Figs. 10, 11). The same heat flux, combined with stronger winds, mixes the water column to greater depths (e.g. 2 May 1983, Figs. 10, 11).

Frequently, the onset of algal blooms is triggered by changes in the vertical mixing patterns. Calm situations are favourable for algal growth, as demonstrated by the occurrence of algal blooms below an ice cover which eliminates most of the kinetic energy input into the water column.

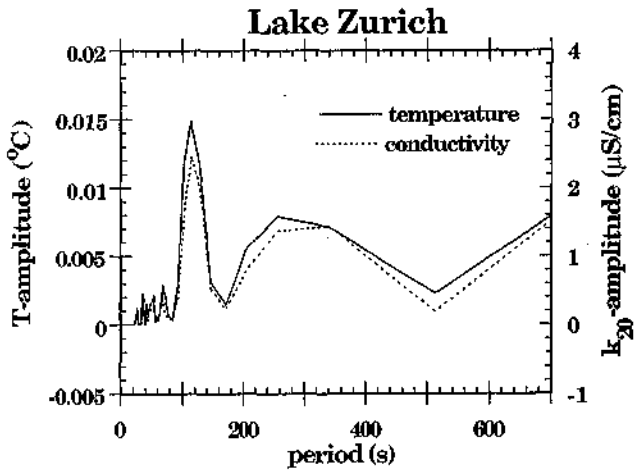


Figure 9. Spectra of fluctuations of temperature (changes in amplitude, °C) and electrical conductivity ( $\mu\text{S cm}^{-1}$  at  $20^\circ\text{C}$ ) measured every second in Lake Zurich (Switzerland). The peak at 100 s represents the stability frequency, a measure for the strength of the vertical density gradient.

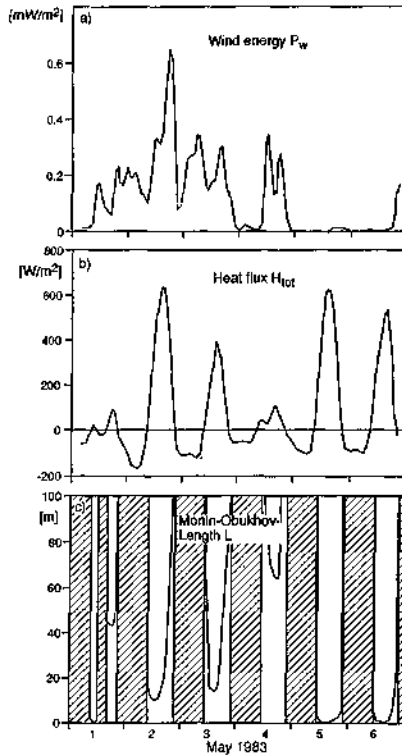


Figure 10. (a) Input of kinetic energy ( $\text{mW m}^{-2}$ ), (b) heat flux ( $\text{Wm}^{-2}$ ) at the water surface (positive if directed into the lake) and (c) the Monin-Obukhov length (m) in Lake Sempach (Switzerland) for 1 May to 6 May 1983. From Marti & Imboden (1986).

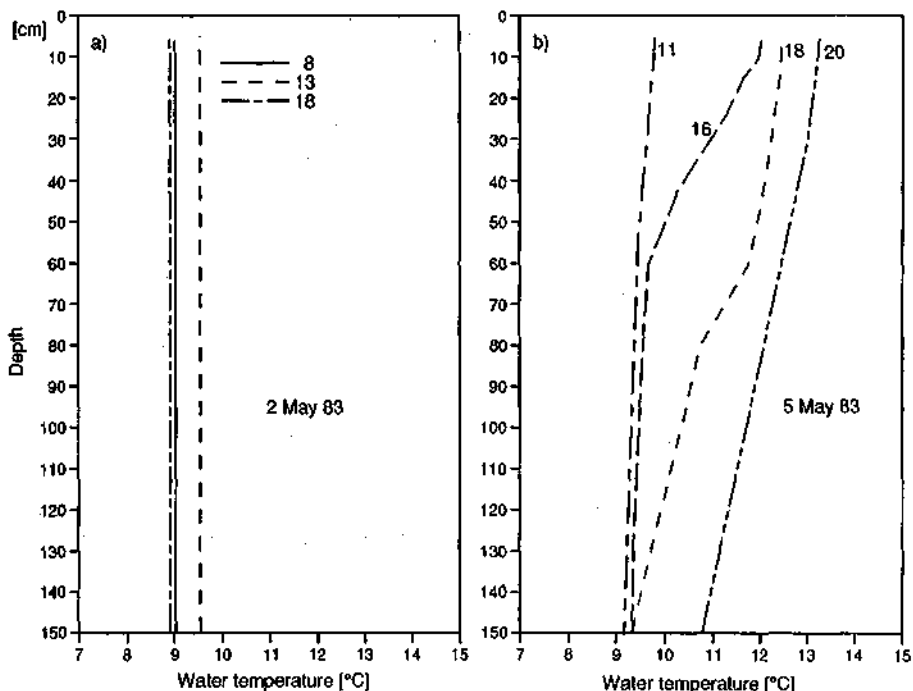


Figure 11. Temporal evolution of the vertical temperature structure in the top 1.5 metres of Lake Sempach (Switzerland) on (a) 2 May 1983 and (b) 5 May 1983. From Marti & Imboden (1986).

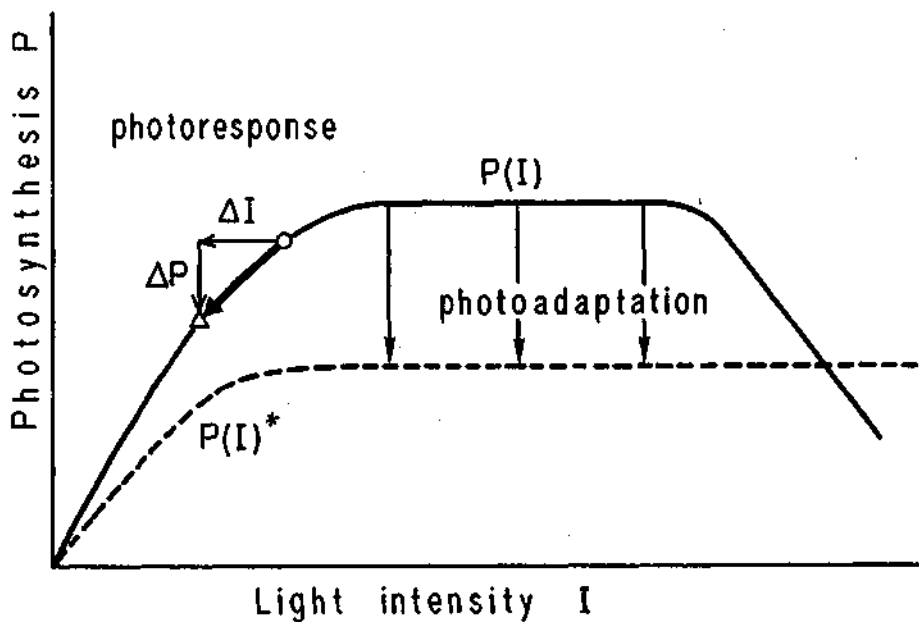


Figure 12. Schematic representation of the relation between rate of photosynthesis,  $P$ , and light intensity,  $I$ . See text for further explanations.

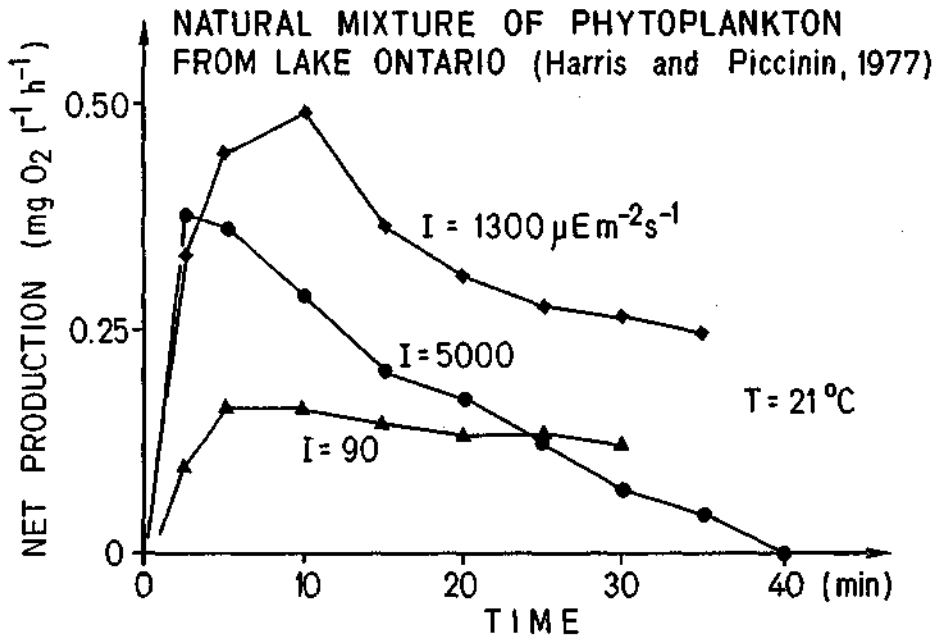


Figure 13. Temporal variation of net photosynthesis at different light intensities for a natural mixture of phytoplankton from Lake Ontario (N. America). In all experiments, the algae were kept in the dark for 5 min and then exposed to different light intensities for periods of 30–40 min at 21°C. Photosynthesis was measured by the rate of oxygen production ( $\text{mg O}_2 \text{l}^{-1} \text{h}^{-1}$ ). From Harris & Piccinin (1977).

### Photoadaptation and photoresponse

The final link between mixing and algal growth is related to the dynamics of photosynthesis ( $P$ ) under changing light intensity ( $I$ ). Figure 12 explains the difference between photoadaptation, the permanent change of the  $P/I$  curve due to long-term changes of the light, and photoresponse, the change  $\Delta P$  along a fixed  $P/I$  curve due to a change of  $\Delta I$  of the light. Of course, this distinction is somewhat artificial. If the time-scale of change in  $I$  is continuously varied, a gradual change from the (reversible) photoresponse to a more permanent (though not really irreversible) photoadaptation can be observed.

As shown by various experiments (e.g. Harris & Piccinin 1977) the  $P/I$  curve is not static. At low intensities the maximum  $P$  is only reached after some minutes (Fig. 13) while at larger values of  $I$ , a significant depletion of  $P$  is observed after some time (photoinhibition).

Pahl-Wostl & Imboden (1990) have developed a mathematical model to describe the dynamic response of  $P$  to changing  $I$ . In Figure 14, this model is applied to phytoplankton suspended in a Langmuir cell (Leibovich 1983). As can be seen, algal growth is favoured by the dynamic response of the plankton to changing light intensity, compared to the exposure of algae to a fixed light intensity.

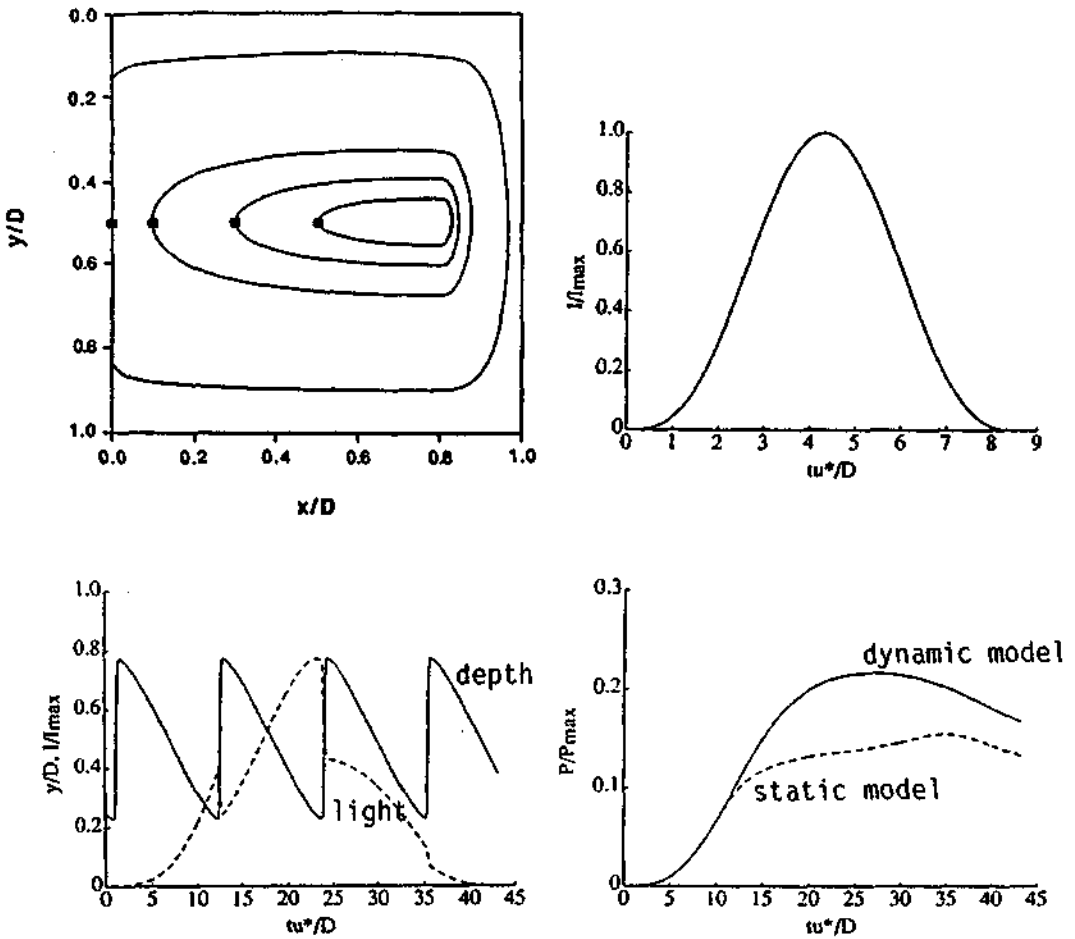


Figure 14. Model responses of phytoplankton suspended in Langmuir cells. Top (left), motion of algae in Langmuir cells while exposed (right) to a diurnal light variation. Below (left), light experienced by an individual cell and (right) the mean photosynthesis of all cells, calculated by a static model and a dynamic model.  $D$  is depth of the Langmuir cell;  $u^*$  is the maximum surface velocity;  $\omega^*/D$  is non-dimensional time;  $I_{max}$  is the surface maximum light intensity. From Patterson (1991).

### Conclusions

Based on theoretical as well as experimental evidence (Lewis *et al.* 1984) it can be concluded that mixing in lakes and oceans must be an important criterion for competing algae. Changes in the mixing pattern must have an influence on the composition of the planktonic community. Although a quantitative understanding of these phenomena does not yet exist, artificial or natural changes of the physical structure of lakes have also to be considered under these aspects.

### References

- Harris, G. P. & Piccinin, B. B. (1977). Photosynthesis by natural phytoplankton populations. *Archiv für Hydrobiologie*, **80**, 405-457.
- Horn, W., Mortimer, C. H. & Schwabe, D. J. (1986). Wind-induced internal seiches in Lake Zürich observed and modelled. *Limnology and Oceanography*, **31**, 1232-1254.
- Imboden, D. M. (1990). Mixing and transport in lakes: mechanisms and ecological relevance. In *Large Lakes: Ecological Structure and Function* (eds. M. Tilzer & C. Serruya), pp. 47-80. Springer, Berlin.
- Imboden, D. M. & Gächter, R. (1978). A dynamic lake model for trophic state prediction. *Ecological Modelling*, **4**, 77-98.
- Imboden, D. M. & Gächter, R. (1979). The impact of physical processes on the trophic state of a lake. In *Biological Aspects of Freshwater Pollution* (ed. O. Ravera), pp. 93-110. Pergamon Press, Oxford.
- Imboden, D. M., Lemming, U., Joller, T. & Schürter, M. (1983). Mixing processes in lakes: mechanisms and ecological relevance. *Schweizerische Zeitschrift für Hydrologie*, **45**, 11-44.
- Imboden, D. M., Stotz, B. & Wilest, A. (1988). Hypolimnetic mixing in a deep alpine lake and the role of a storm event. *Verhandlungen der Internationale Vereinigung für Theoretische und Angewandte Limnologie*, **23**, 67-73.
- Leibovich, S. (1983). The form and dynamics of Langmuir circulations. *Annual Reviews of Fluid Mechanics*, **15**, 391-427.
- Lewis, M. R., Horne, E. P. W., Cullen, J. J., Oakey, N. S. & Platt, T. (1984). Turbulent motions may control phytoplankton photosynthesis in the upper ocean. *Nature*, **311**, 49-50.
- Marti, D. E. & Imboden, D. M. (1986). Thermische Energieflüsse an der Wasseroberfläche: Beispiel Sempachersee. *Zeitschrift für Hydrologie*, **48**, 196-229.
- Mortimer, C. H. (1974). Lake hydrodynamics. *Mitteilungen Internationale Vereinigung für Theoretische und Angewandte Limnologie*, **20**, 124-197.
- Pahl-Wostl, C. & Imboden, D. M. (1990). DYPHORA – A dynamic model for the rate of photosynthesis of algae. *Journal of Plankton Research*, **12**, 351-369.
- Patterson, J. C. (1991). Modelling the effects of motion on primary production in the mixed layer of lakes. *Aquatic Sciences*, **53**, 218-238.
- Vollenweider, R. & Kerekes, J. (1982). *Eutrophication of waters, monitoring assessment, control*. OECD, Paris.